

Supporting Information

Enhancing the single-molecule magnet performance of δ -diketonate Dy(III) complexes by modulating the coordination microenvironment and magnetic interaction: from mononuclear to dinuclear structure

Yafu Wang,^{a#} Zhaopeng Zeng,^{a, c#} Shuchang Luo,^{*b} Yan Guo^a and Xiangyu Liu^{*a}

^aState Key Laboratory of High-Efficiency Utilization of Coal and Green Chemical Engineering, College of Chemistry and Chemical Engineering, Ningxia University, Yinchuan 750021, China.

^bCollege of Chemical Engineering, Guizhou University of Engineering Science, Bijie 551700, China.

^cXinhua College of Ningxia University, Yinchuan 750021, China.

These authors contributed equally to this work.

*Corresponding author

Prof. Xiangyu Liu

E-mail: xiangyuli432@126.com

Dr. Shuchang Luo

Email: luosc@gues.edu.cn

Contents

1.*Ab initio* calculational details

2.Electronic structure calculations

3.Evaluation of the exchange interactions

Table S1. Crystal data and structure refinement details for complexes **1-3**.

Table S2. Selected bond lengths (\AA) and bond angles ($^\circ$) for **1-3**.

Table S3. Continuous Shape Measurements (CShMs) for Dy(III) ions in **1** and **2** by SHAPE 2.1.

Table S4. Relaxation fitting parameters from least-squares fitting of $\chi(f)$ data under 0 Oe dc field of **2**.

Table S5. Relaxation fitting parameters from least-squares fitting of $\chi(f)$ data under 0 Oe dc field of **1@Y**.

Table S6. Calculated energy levels (cm^{-1}) and g (g_x , g_y , g_z) tensors and τ_{QTM} (s^{-1}) of the lowest eight Kramers doublets (KDs) of **1**, **2a** and **2b** using CASSCF/RASSI-SO with OpenMolcas.

Table S7. Wave functions with definite projection of the total moment $| m_j \rangle$ for the lowest eight KDs of **1**, **2a** and **2b** using CASSCF/RASSI-SO with OpenMolcas.

Table S8. Mulliken atomic charge on the metal atoms and donor atoms in the ground state of complexes **1**, **2a** and **2b** calculated within CASSCF.

Table S9. Calculated crystal field parameters B (k , q) for **1**, **2a** and **2b** using SCF/RASSI-SO with OpenMolcas.

Fig. S1 Crystal packing diagram for complex **1**, the dashed line represents the interaction.

Fig. S2 Crystal packing diagram for complex **2**, the dashed line represents the interaction.

Fig. S3 PXRD curves of **1**, **3**, **1@Y** (a) and **2** (b).

Fig. S4 Plots of M vs H/T for **1** (a) and **2** (b) at different temperatures.

Fig. S5 Ac magnetic susceptibility measurements for **1** (a) in zero static field. Frequency dependence of χ''_M susceptibilities for **1** (b) under different dc fields.

Fig. S6 Temperature dependence of the χ'_M (a) and χ''_M (b) ac susceptibilities for complex **2** at different frequencies under zero static field.

Fig. S7 Frequency dependence of the χ'_M ac susceptibilities for **1@Y** under zero static field.

Fig. S8 Mulliken spin density of complexes **1** (a), **2a** (b) and **2b** (c) (magenta for α spin, green for β spin, isovalue = 0.02).

References

1. Ab initio calculational details

The SA-CASSCF/RASSI-SO methodology for complexes **1**, **2a** and **2b** were performed in OpenMolcas software [1] based on the crystal structures obtained from experimental X-ray structures. The calculated data were visualized with the VMD 1.9.3 program [2]. Due to the limitations of our hardware, the calculations were performed with the Dy atoms in the ANO-RCC-VTZP basis set, the O and N atoms in the ANO-RCC-VTZ basis sets, and the other atoms in the ANO-RCC-MB basis sets [3]. The relativistic effect uses the DKH2 Hamiltonian function include 9 electrons in the 7 4f orbitals [4]. All 21 sextet, 224 quartet and 490 doublet states were considered in three separate calculations. The SOC operator is composed of 21 sextet, 128 quartet and 130 doublet states.

2. Electronic structure calculations

To further understand the slow relaxation mechanism for **1**, **2a** and **2b**, *ab initio* calculations were performed under SA-CASSCF/RASSI-SO/SINGLE_ANISO module by OpenMolcas program [1]. The calculations show that the **1**, **2a** and **2b** Kramers double states (KDs) have large differences with energies of 4166.751 cm^{-1} (**1**), 594.822 cm^{-1} (**2a**) and 594.729 cm^{-1} (**2b**) (Table S6). **2a** and **2b** have similar coordination environments and their calculated energy barriers are almost the same.

3. Evaluation of the exchange interactions

To evaluate the magnetic interactions of the complex **2**, we calculate their coupling constants in three steps. First, the model complexes **2a** and **2b** were obtained by replacing one of the Dy(III) ion of the binuclear complexes with the antimagnetic Lu(III) ion, and the corresponding magnetic data were calculated by SA-CASSCF/RASSI-SO/SINGLE_ANISO method. Second, the Dy(III) ($S = 5/2$) ion was replaced with the isotropic Gd(III) ($S = 7/2$) ion to obtain the dinuclear Gd(III) complexes, and based on the broken symmetry DFT method using ORCA 5.0.3 software [5-7], the energies were calculated broken symmetry state ($M_s = 0$) and the high-spin state ($M_s = 7$) at the B3LYP/DKH2-def2-SVP level of theory (the SARC2-DKH-QZVP basis sets for Gd atoms) (it's Hamiltonian operator and magnetic coupling constant calculations can be expressed in Eq. (1-3)) [8], and the exchange coupling constant $J_{\text{exchang,Gd-Gd}}$ is obtained by using Eq. (2). The second-order Douglas-Kroll-Hess relativistic effect is considered [9,10]. The exchange coupling constants $J_{\text{exchang,Dy-Dy}}$ for the dinuclear Dy complexes are further calculated by using Eq. (3) [11].

$$\hat{H} = -J_{\text{exchange,Gd-Gd}} \hat{S}_{Gd1} \cdot \hat{S}_{Gd2} \quad (1)$$

$$J_{\text{exchange,Gd-Gd}} = \frac{8(E_{BS} - E_{HS})}{49} \quad (2)$$

$$J_{\text{exchange,Dy-Dy}} = \frac{(7/2)^2}{(5/2)^2} J_{\text{exchange,Gd-Gd}} = \frac{49}{25} J_{\text{exchange,Gd-Gd}} \quad (3)$$

Here, E_{BS} and E_{HS} denote the energies of the symmetry-broken and high-spin states, respectively.

Finally, based on the Lines model, the dipolar-dipolar magnetic coupling constants (J_{dipolar}) and total magnetic coupling constants (J_{total}) of the binuclear complex **2** are calculated by equation (4-6), and the results are shown in Table 1 [10].

$$\hat{H} = -J_{\text{total}} \hat{S}_{Dy1} \cdot \hat{S}_{Dy2} \quad (4)$$

$$J_{\text{total}} = J_{\text{dipolar}} + J_{\text{exchange,Dy-Dy}} \quad (5)$$

$$J_{\text{dipolar}} = -\frac{\mu_B^2 g_{1z} g_{2z}}{r^3} (\cos\theta - 3\cos\phi_1 \cos\phi_2) \quad (6)$$

where ϑ is the angle between the ground magnetic axes of the two Dy(III) ions, ϕ_1 and ϕ_2 denote the angle between the ground magnetic axes of Dy1, Dy2 and the Dy-Dy line, respectively. the values of g_{1z} and g_{2z} are g_z for the ground doublet states of Dy1, Dy2, respectively, and r is the distance between the two Dy ions, $\mu_B^2 = 0.43297\text{ cm}^{-1}/\text{T}$.

Table S1. Crystal data and structure refinement details for complexes **1-3**.

complex	1	2	3
Empirical formula	C ₄₉ H ₅₃ DyN ₂ O ₆	C ₄₃ H ₄₈ DyN ₂ O ₆	C ₄₉ H ₅₃ YN ₂ O ₆
Formula weight	928.43	851.33	854.84
Crystal system	hexagonal	triclinic	hexagonal
Space group	P6 ₁	P $\overline{1}$	P6 ₅
Temperature(K)	300.15	300.0	300.0
<i>a</i> (Å)	12.3790(7)	12.4689(18)	12.3509(2)
<i>b</i> (Å)	12.3790(7)	12.5848(17)	12.3509(2)
<i>c</i> (Å)	51.501(4)	15.1880(18)	51.4803(16)
α (°)	90	104.710(4)	90
β (°)	90	90.508(4)	90
γ (°)	120	116.886(4)	120
<i>V</i> (Å ³)	6834.7(9)	2034.7(5)	6800.9(3)
<i>Z</i>	6	2	6
μ (mm ⁻¹)	1.688	1.883	1.335
Unique reflections	9181	7586	7512
Observed reflections	59205	32561	23392
<i>R</i> _{int}	0.0356	0.0266	0.0504
<i>R</i> ₁ , <i>wR</i> ₂ [<i>I</i> > 2σ(<i>I</i>)]	<i>R</i> ₁ = 0.0207, <i>wR</i> ₂ = 0.0436	<i>R</i> ₁ = 0.0209, <i>wR</i> ₂ = 0.0496	<i>R</i> ₁ = 0.0519, <i>wR</i> ₂ = 0.1294
<i>R</i> ₁ , <i>wR</i> ₂ (all data)	<i>R</i> ₁ = 0.0234, <i>wR</i> ₂ = 0.0445	<i>R</i> ₁ = 0.0240, <i>wR</i> ₂ = 0.0512	<i>R</i> ₁ = 0.0700, <i>wR</i> ₂ = 0.1379

Table S2. Selected bond lengths (\AA) and bond angles ($^\circ$) for **1-3**.

Complex 1			
Dy(1)-O(1)	2.335(3)	O(3)-Dy(1)-N(1)	135.53(11)
Dy(1)-O(2)	2.316(3)	O(3)-Dy(1)-N(2)	79.60(10)
Dy(1)-O(3)	2.324(3)	O(4)-Dy(1)-O(1)	141.45(10)
Dy(1)-O(4)	2.333(3)	O(4)-Dy(1)-N(1)	76.85(11)
Dy(1)-O(5)	2.307(3)	O(4)-Dy(1)-N(2)	75.31(10)
Dy(1)-O(6)	2.321(3)	O(5)-Dy(1)-O(1)	79.70(9)
Dy(1)-N(1)	2.563(3)	O(5)-Dy(1)-O(2)	80.40(10)
Dy(1)-N(2)	2.575(3)	O(5)-Dy(1)-O(3)	80.38(10)
O(1)-Dy(1)-N(1)	116.64(11)	O(5)-Dy(1)-O(4)	112.77(11)
O(1)-Dy(1)-N(2)	80.02(10)	O(5)-Dy(1)-O(6)	72.67(10)
O(2)-Dy(1)-O(1)	72.77(10)	O(5)-Dy(1)-N(1)	141.86(11)
O(2)-Dy(1)-O(3)	145.03(10)	O(5)-Dy(1)-N(2)	154.48(10)
O(2)-Dy(1)-O(4)	143.25(11)	O(6)-Dy(1)-O(1)	144.56(10)
O(2)-Dy(1)-O(6)	80.99(11)	O(6)-Dy(1)-O(3)	120.12(11)
O(2)-Dy(1)-N(1)	73.21(11)	O(6)-Dy(1)-O(4)	71.58(11)
O(2)-Dy(1)-N(2)	108.00(10)	O(6)-Dy(1)-N(1)	76.36(11)
O(3)-Dy(1)-O(1)	75.23(10)	O(6)-Dy(1)-N(2)	131.71(10)
O(3)-Dy(1)-O(4)	71.55(10)	N(1)-Dy(1)-N(2)	62.44(11)

Complex 2			
Dy(1)-N(1)	2.6199(19)	O(3)-Dy(1)-O(2)	77.50(6)
Dy(1)-N(2) ¹	2.628(2)	O(3)-Dy(1)-O(6)	146.74(6)
Dy(1)-O(1)	2.3353(17)	O(4)-Dy(1)-N(1)	72.18(6)
Dy(1)-O(2)	2.3155(16)	O(4)-Dy(1)-N(2) ¹	103.19(7)
Dy(1)-O(3)	2.3149(17)	O(4)-Dy(1)-O(1)	137.53(6)
Dy(1)-O(4)	2.3060(17)	O(4)-Dy(1)-O(2)	149.62(6)
Dy(1)-O(5)	2.2764(15)	O(4)-Dy(1)-O(3)	73.47(6)
Dy(1)-O(6)	2.3225(17)	O(4)-Dy(1)-O(6)	79.61(7)
N(1)-Dy(1)-N(2) ¹	61.46(6)	O(5)-Dy(1)-N(1)	145.62(6)
O(1)-Dy(1)-N(1)	69.84(6)	O(5)-Dy(1)-N(2) ¹	151.03(6)
O(1)-Dy(1)-N(2) ¹	74.45(7)	O(5)-Dy(1)-O(1)	118.64(7)
O(2)-Dy(1)-N(1)	128.20(6)	O(5)-Dy(1)-O(2)	84.11(6)
O(2)-Dy(1)-N(2) ¹	75.43(6)	O(5)-Dy(1)-O(3)	84.20(6)
O(2)-Dy(1)-O(1)	72.14 (6)	O(5)-Dy(1)-O(4)	84.27(6)
O(2)-Dy(1)-O(6)	123.41(7)	O(5)-Dy(1)-O(6)	73.89(6)
O(3)-Dy(1)-N(1)	111.46(6)	O(6)-Dy(1)-N(1)	77.42(6)
O(3)-Dy(1)-N(2) ¹	71.62(6)	O(6)-Dy(1)-N(2) ¹	134.74(6)
O(3)-Dy(1)-O(1)	138.96(6)	O(6)-Dy(1)-O(1)	74.27(6)

¹1-X,1-Y,1-Z

Complex 3			
Y(1)-N(1)	2.559(6)	O(3)-Y(1)-N(2)	131.93(19)
Y(1)-N(2)	2.561(6)	O(3)-Y(1)-O(1)	120.3(2)
Y(1)-O(1)	2.317(5)	O(3)-Y(1)-O(2)	71.59(19)
Y(1)-O(2)	2.322(6)	O(3)-Y(1)-O(5)	80.7(2)
Y(1)-O(3)	2.305(5)	O(3)-Y(1)-O(6)	144.77(18)
Y(1)-O(4)	2.297(5)	O(4)-Y(1)-N(1)	142.3(2)
Y(1)-O(5)	2.306(5)	O(4)-Y(1)-N(2)	153.91(19)
Y(1)-O(6)	2.320(5)	O(4)-Y(1)-O(1)	80.31(18)
N(1)-Y(1)-N(2)	62.6(2)	O(4)-Y(1)-O(2)	113.0(2)
O(1)-Y(1)-N(1)	135.36(19)	O(4)-Y(1)-O(3)	73.03(19)
O(1)-Y(1)-N(2)	79.43(19)	O(4)-Y(1)-N(5)	80.75(19)
O(1)-Y(1)-O(2)	71.72(19)	O(4)-Y(1)-N(6)	79.80(18)
O(1)-Y(1)-O(6)	75.30(19)	O(5)-Y(1)-N(1)	73.1(2)
O(2)-Y(1)-O(6)	80.99(11)	O(5)-Y(1)-N(2)	107.9(2)
O(2)-Y(1)-N(1)	76.5(2)	O(5)-Y(1)-O(1)	145.33(19)
O(2)-Y(1)-N(2)	75.41(19)	O(5)-Y(1)-O(2)	142.8(2)
O(2)-Y(1)-O(6)	141.44(18)	O(5)-Y(1)-O(6)	73.02(19)
O(3)-Y(1)-N(1)	76.2(2)	O(6)-Y(1)-N(1)	116.5(2)
O(6)-Y(1)-N(2)	79.46(18)		

Table S3. Continuous Shape Measurements (CShMs) for Dy(III) ions in **1** and **2** by SHAPE 2.1.

Configuration	ABOXIY, 1	ABOXIY, 2(Dy1)	ABOXIY, 2(Dy2)
Hexagonal bipyramid (D_{6h})	15.947	16.517	16.512
Cube (O_h)	9.683	10.285	10.276
Square antiprism (D_{4d})	0.617	0.583	0.584
Triangular dodecahedron (D_{2d})	2.406	2.087	2.083
Johnson elongated triangular bipyramid J14 (D_{3h})	26.273	27.209	27.209
Biaugmented trigonal prism J50 (C_{2v})	2.741	2.543	2.547
Biaugmented trigonal prism (C_{2v})	2.222	1.939	1.941
Snub disphenoid J84 (D_{2d})	4.793	4.794	4.793
Triakis tetrahedron (T_d)	10.492	11.002	10.993
Elongated trigonal bipyramidal (D_{3h})	22.529	23.378	23.379

Table S4. Relaxation fitting parameters from least-squares fitting of $\chi(f)$ data under 0 Oe dc field of **2**.

$T(K)$	χ_T	χ_s	α
7	8.580	0.533	0.145
8	7.389	0.429	0.093
9	6.519	0.338	0.062
10	5.853	0.272	0.042
11	5.325	0.232	0.028
12	4.874	0.188	0.020
13	4.504	0.166	0.014
14	4.201	0.154	0.011
15	3.926	0.184	0.003
16	3.692	0.172	0.005
17	3.481	0.148	0.006
18	3.293	0.246	0.006
19	3.118	0.293	4.74×10^{-15}
20	2.968	0.531	4.23×10^{-17}

Table S5. Relaxation fitting parameters from least-squares fitting of $\chi(f)$ data under 0 Oe dc field of **1@Y**.

$T(K)$	χ_T	χ_s	α
4	2.086	0.172	0.080
4.5	2.224	0.210	0.086
5	2.385	0.203	0.124
5.5	2.594	0.239	0.145
6	2.814	0.274	0.170
6.5	3.097	0.301	0.219
7	3.435	0.335	0.263
7.5	3.873	0.306	0.346
8	4.617	0.345	0.428

Table S6. Calculated energy levels (cm^{-1}) and g (g_x , g_y , g_z) tensors and τ_{QTM} (s^{-1}) of the lowest eight Kramers doublets (KDs) of **1**, **2a** and **2b** using CASSCF/RASSI-SO with OpenMolcas.

KDs	E/cm^{-1}	g_x	g_y	g_z	g_z Angle/ $^\circ$	$\tau_{\text{QTM}} \text{s}^{-1}$	
1	ground	0.000	1.5015	6.0670	13.9234	--	1.396×10^{-9}
	1st	345.910	3.6047	4.1533	4.9253	90.40	8.720×10^{-10}
	2nd	1054.872	0.2795	0.2997	8.4109	90.04	1.791×10^{-7}
	3rd	2369.779	0.0097	0.0190	10.9284	90.32	8.579×10^{-5}
	4th	3537.194	8.7755	7.4733	1.6388	90.07	3.130×10^{-10}
	5th	3702.952	0.2193	0.4772	12.1302	91.70	1.573×10^{-7}
	6th	3752.888	0.2334	1.3301	5.4133	87.67	1.093×10^{-8}
	7th	4166.751	0.8705	0.8984	7.5768	--	1.753×10^{-8}
2a	ground	0.000	0.0098	0.0109	19.4226	--	3.229×10^{-4}
	1st	151.469	0.3914	0.6505	15.7314	166.77	9.762×10^{-8}
	2nd	233.666	1.0442	1.6776	12.4596	158.09	1.154×10^{-8}
	3rd	282.180	9.0121	6.6287	3.7047	65.98	3.364×10^{-10}
	4th	327.249	1.1516	4.2735	8.5987	98.45	1.764×10^{-9}
	5th	350.751	1.7941	5.2685	14.5189	72.98	1.793×10^{-9}
	6th	506.816	0.0187	0.0234	16.1930	61.31	6.447×10^{-5}
	7th	594.822	0.0007	0.0130	18.3468	62.09	3.867×10^{-4}
2b	ground	0.000	0.0097	0.0108	19.4237	--	3.293×10^{-4}
	1st	151.513	0.3906	0.6491	15.7339	166.77	9.805×10^{-8}
	2nd	233.719	1.0457	1.6796	12.4626	149.76	1.152×10^{-8}
	3rd	282.248	9.0119	6.6316	3.7042	73.91	3.363×10^{-10}
	4th	327.277	1.1352	4.2810	8.5976	103.17	1.761×10^{-9}
	5th	350.779	1.7901	5.2470	14.5410	109.10	1.809×10^{-9}
	6th	506.757	0.0189	0.0236	16.1917	68.76	6.327×10^{-5}
	7th	594.729	0.0007	0.0130	18.3454	68.37	3.867×10^{-4}

Table S7. Wave functions with definite projection of the total moment $| m_j \rangle$ for the lowest eight KDs of **1**, **2a** and

2b using CASSCF/RASSI-SO with OpenMolcas.

E/cm^{-1}		wave functions
0.000		64.9% $ \pm 15/2\rangle + 1.8\% \pm 13/2\rangle + 18.2\% \pm 9/2\rangle + 1.4\% \pm 7/2\rangle + 4.3\% \pm 5/2\rangle + 8.5\% \pm 1/2\rangle$
345.910		16.8% $ \pm 15/2\rangle + 31.5\% \pm 13/2\rangle + 5.6\% \pm 11/2\rangle + 1.7\% \pm 7/2\rangle + 29.0\% \pm 5/2\rangle + 1.2\% \pm 3/2\rangle + 13.3\% \pm 1/2\rangle$
1054.872		10.7% $ \pm 15/2\rangle + 30.5\% \pm 13/2\rangle + 3.9\% \pm 11/2\rangle + 24.8\% \pm 9/2\rangle + 1.4\% \pm 7/2\rangle + 5.3\% \pm 3/2\rangle + 23.2\% \pm 1/2\rangle$
2369.779		3.5% $ \pm 15/2\rangle + 18.2\% \pm 13/2\rangle + 1.3\% \pm 11/2\rangle + 39.2\% \pm 9/2\rangle + 32.1\% \pm 5/2\rangle + 5.3\% \pm 1/2\rangle$
1	3537.194	2.7% $ \pm 13/2\rangle + 50.9\% \pm 11/2\rangle + 12.8\% \pm 7/2\rangle + 31.4\% \pm 3/2\rangle$
3702.952		3.9% $ \pm 13/2\rangle + 4.6\% \pm 11/2\rangle + 13.8\% \pm 9/2\rangle + 6.0\% \pm 7/2\rangle + 28.9\% \pm 5/2\rangle + 3.8\% \pm 3/2\rangle + 38.3\% \pm 1/2\rangle$
3752.888		1.5% $ \pm 15/2\rangle + 5.9\% \pm 13/2\rangle + 27.0\% \pm 11/2\rangle + 1.6\% \pm 9/2\rangle + 45.0\% \pm 7/2\rangle + 4.7\% \pm 5/2\rangle + 6.6\% \pm 3/2\rangle + 7.7\% \pm 1/2\rangle$
4166.751		1.4% $ \pm 15/2\rangle + 5.7\% \pm 13/2\rangle + 6.3\% \pm 11/2\rangle + 1.0\% \pm 9/2\rangle + 31.5\% \pm 7/2\rangle + 51.3\% \pm 3/2\rangle + 2.5\% \pm 1/2\rangle$
0.000		92.6% $ \pm 15/2\rangle + 5.9\% \pm 11/2\rangle$
151.469		72.7% $ \pm 13/2\rangle + 1.5\% \pm 11/2\rangle + 16.6\% \pm 9/2\rangle + 4.3\% \pm 7/2\rangle + 3.0\% \pm 5/2\rangle + 1.4\% \pm 3/2\rangle$
233.666		4.0% $ \pm 15/2\rangle + 9.7\% \pm 13/2\rangle + 36.2\% \pm 11/2\rangle + 4.3\% \pm 9/2\rangle + 18.9\% \pm 7/2\rangle + 8.8\% \pm 5/2\rangle + 10.5\% \pm 3/2\rangle + 7.6\% \pm 1/2\rangle$
282.180		2.1% $ \pm 13/2\rangle + 24.9\% \pm 11/2\rangle + 16.9\% \pm 9/2\rangle + 2.4\% \pm 7/2\rangle + 11.4\% \pm 5/2\rangle + 11.9\% \pm 3/2\rangle + 29.7\% \pm 1/2\rangle$
2a	327.249	4.8% $ \pm 13/2\rangle + 5.2\% \pm 11/2\rangle + 24.3\% \pm 9/2\rangle + 27.2\% \pm 7/2\rangle + 4.7\% \pm 5/2\rangle + 19.3\% \pm 3/2\rangle + 14.2\% \pm 1/2\rangle$
350.751		1.2% $ \pm 13/2\rangle + 3.2\% \pm 11/2\rangle + 4.8\% \pm 9/2\rangle + 18.0\% \pm 7/2\rangle + 46.4\% \pm 5/2\rangle + 21.7\% \pm 3/2\rangle + 4.4\% \pm 1/2\rangle$
506.816		1.3% $ \pm 15/2\rangle + 6.2\% \pm 13/2\rangle + 15.4\% \pm 11/2\rangle + 18.3\% \pm 9/2\rangle + 7.6\% \pm 7/2\rangle + 3.6\% \pm 5/2\rangle + 17.9\% \pm 3/2\rangle + 29.9\% \pm 1/2\rangle$
594.822		3.2% $ \pm 13/2\rangle + 7.7\% \pm 11/2\rangle + 14.1\% \pm 9/2\rangle + 21.1\% \pm 7/2\rangle + 22.2\% \pm 5/2\rangle + 17.2\% \pm 3/2\rangle + 13.9\% \pm 1/2\rangle$
0.000		92.6% $ \pm 15/2\rangle + 5.9\% \pm 11/2\rangle$
151.513		72.7% $ \pm 13/2\rangle + 1.5\% \pm 11/2\rangle + 16.5\% \pm 9/2\rangle + 4.4\% \pm 7/2\rangle + 3.0\% \pm 5/2\rangle + 1.4\% \pm 3/2\rangle$
233.719		4.1% $ \pm 15/2\rangle + 9.7\% \pm 13/2\rangle + 36.2\% \pm 11/2\rangle + 4.2\% \pm 9/2\rangle + 18.9\% \pm 7/2\rangle + 8.7\% \pm 5/2\rangle + 10.4\% \pm 3/2\rangle + 7.6\% \pm 1/2\rangle$
282.248		2.1% $ \pm 13/2\rangle + 25.0\% \pm 11/2\rangle + 16.9\% \pm 9/2\rangle + 2.4\% \pm 7/2\rangle + 11.3\% \pm 5/2\rangle + 11.9\% \pm 3/2\rangle + 29.6\% \pm 1/2\rangle$
2b	327.277	4.8% $ \pm 13/2\rangle + 5.2\% \pm 11/2\rangle + 24.3\% \pm 9/2\rangle + 27.1\% \pm 7/2\rangle + 4.7\% \pm 5/2\rangle + 19.4\% \pm 3/2\rangle + 14.2\% \pm 1/2\rangle$
350.779		1.1% $ \pm 13/2\rangle + 3.1\% \pm 11/2\rangle + 4.9\% \pm 9/2\rangle + 18.1\% \pm 7/2\rangle + 46.3\% \pm 5/2\rangle + 21.7\% \pm 3/2\rangle + 4.4\% \pm 1/2\rangle$
506.757		1.1% $ \pm 15/2\rangle + 6.2\% \pm 13/2\rangle + 15.4\% \pm 11/2\rangle + 18.3\% \pm 9/2\rangle + 7.6\% \pm 7/2\rangle + 3.6\% \pm 5/2\rangle + 17.9\% \pm 3/2\rangle + 29.8\% \pm 1/2\rangle$
594.729		3.2% $ \pm 13/2\rangle + 7.7\% \pm 11/2\rangle + 14.1\% \pm 9/2\rangle + 21.2\% \pm 7/2\rangle + 22.2\% \pm 5/2\rangle + 17.2\% \pm 3/2\rangle + 13.9\% \pm 1/2\rangle$

Table S8. Mulliken atomic charge on the metal atoms and donor atoms in the ground state of complexes **1**, **2a** and

2b calculated within CASSCF.

	1		2a		2b
Dy	1.7629	Dy1	1.7629	Dy2	1.7600
O1	-0.6048	O1	-0.5818	O1'	-0.5808
O2	-0.6023	O2	-0.6015	O2'	-0.6013
O3	-0.5876	O3	-0.6267	O3'	-0.6264
O4	-0.5786	O4	-0.6179	O4'	-0.6186
O5	-0.5945	O5	-0.6037	O5'	-0.6027
O6	-0.5699	O6	-0.5960	O6'	-0.5959
N1	-0.5194	N1	-0.5785	N1'	-0.5369
N2	-0.5374	N2	-0.5635	N2'	-0.5632

Table S9. Calculated crystal field parameters $B(k, q)$ for **1**, **2a** and **2b** using SCF/RASSI-SO with OpenMolcas.

k	q	$B_{k,q}$		
		1	2a	2b
2	-2	-3.30×10^{-1}	-2.05	1.14
2	-1	9.14	2.99	9.00
2	0	-12.61	-2.02	-4.48
2	1	-8.07	-1.25	4.28
2	2	-1.31	-8.92×10^{-1}	-5.19
4	-4	5.70×10^{-2}	-1.50×10^{-2}	1.01×10^{-1}
4	-3	-9.22×10^{-2}	-5.26×10^{-2}	4.66×10^{-2}
4	-2	6.42×10^{-3}	2.26×10^{-3}	1.92×10^{-1}
4	-1	4.06×10^{-2}	-2.12×10^{-3}	-2.76×10^{-3}
4	0	-3.92×10^{-2}	-3.93×10^{-3}	-2.25×10^{-2}
4	1	-1.18×10^{-1}	1.50×10^{-2}	1.25×10^{-1}
4	2	2.00×10^{-2}	-2.79×10^{-2}	-3.24×10^{-2}
4	3	-2.06×10^{-1}	1.36×10^{-2}	-2.64×10^{-1}
4	4	4.86×10^{-2}	-2.81×10^{-3}	9.01×10^{-3}
6	-6	2.76×10^{-5}	2.83×10^{-5}	-4.87×10^{-3}
6	-5	-2.55×10^{-3}	-2.00×10^{-5}	-3.44×10^{-5}
6	-4	1.75×10^{-3}	3.67×10^{-5}	-2.54×10^{-3}
6	-3	-1.57×10^{-3}	-2.44×10^{-4}	7.11×10^{-3}
6	-2	-1.47×10^{-5}	-1.29×10^{-4}	1.01×10^{-4}
6	-1	-7.97×10^{-4}	-1.36×10^{-4}	-9.41×10^{-4}
6	0	-4.05×10^{-5}	-6.99×10^{-6}	-3.36×10^{-4}
6	1	1.84×10^{-3}	-5.35×10^{-5}	-3.13×10^{-3}
6	2	-2.61×10^{-4}	5.93×10^{-5}	-2.42×10^{-3}
6	3	4.67×10^{-3}	-1.55×10^{-4}	-3.02×10^{-3}
6	4	-2.17×10^{-3}	1.47×10^{-4}	-2.42×10^{-3}
6	5	3.18×10^{-3}	-8.17×10^{-5}	3.84×10^{-3}
6	6	5.10×10^{-4}	-1.98×10^{-4}	7.85×10^{-4}

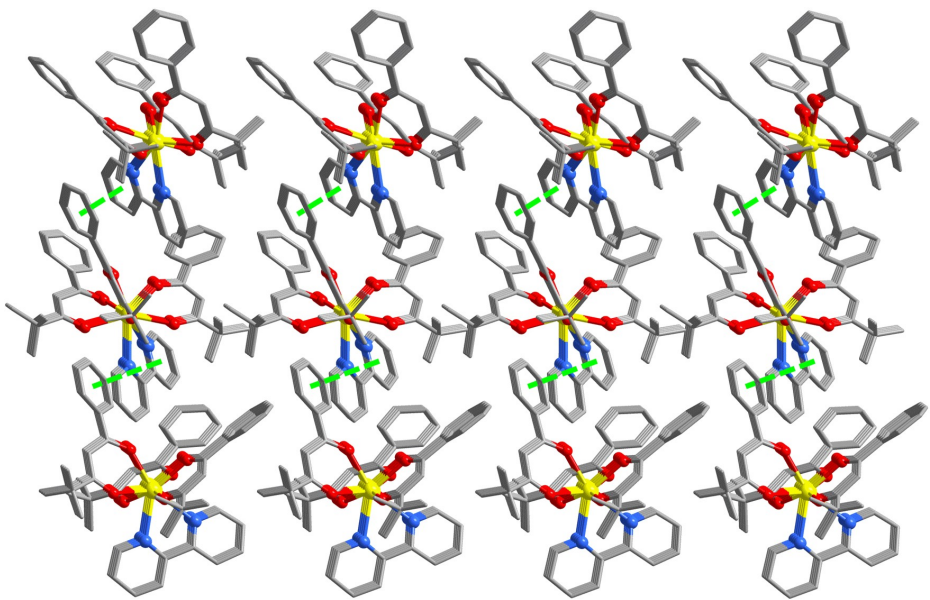


Fig. S1 Crystal packing diagram for complex **1**, the dashed line represents the interaction.

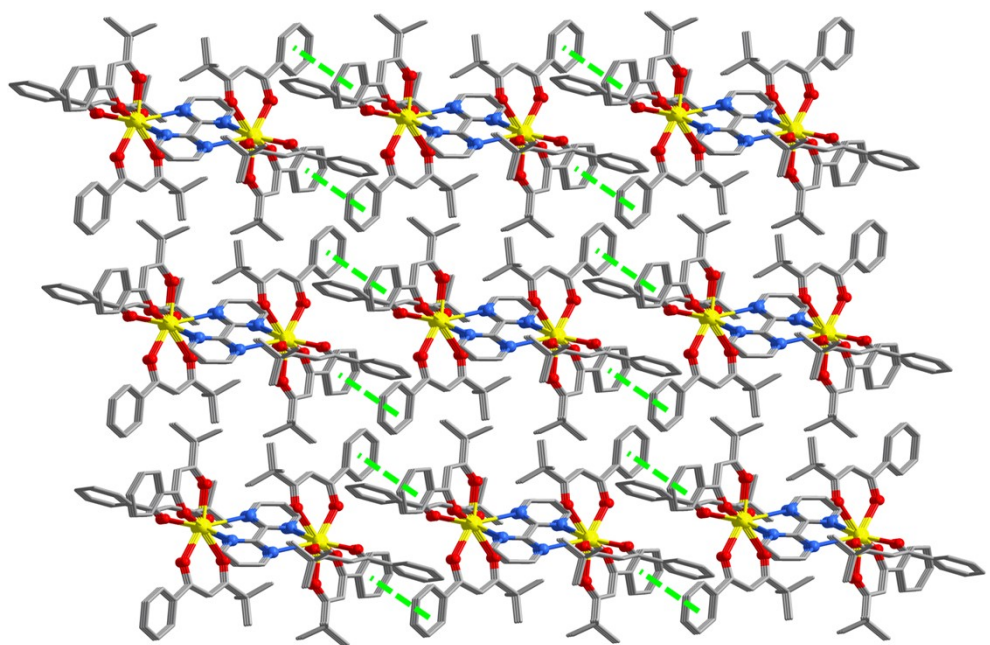


Fig. S2 Crystal packing diagram for complex **2**, the dashed line represents the interaction.

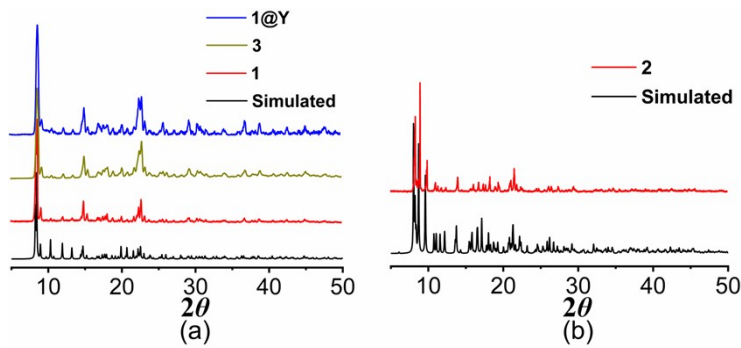


Fig. S3 PXRD curves of **1**, **3**, **1@Y** (a) and **2** (b).

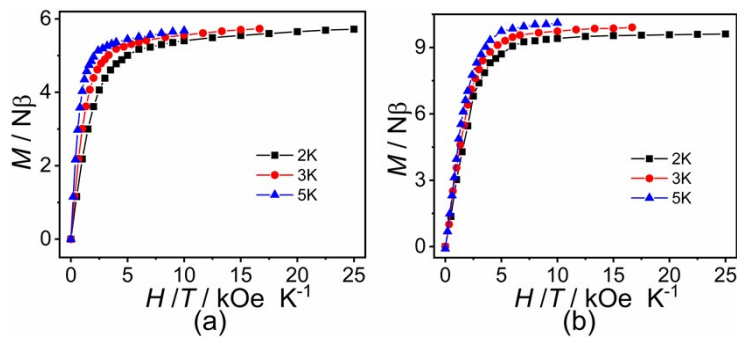


Fig. S4 Plots of M vs H/T for **1** (a) and **2** (b) at different temperatures.

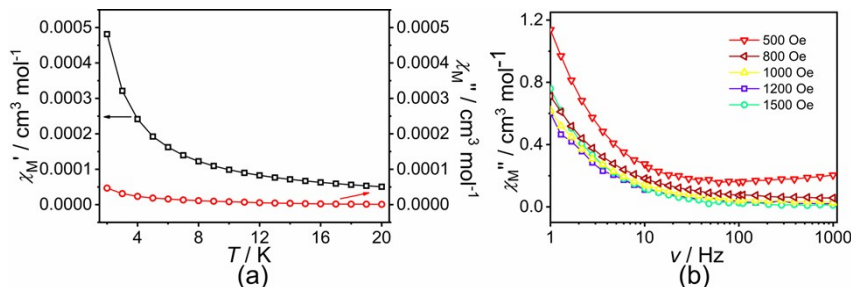


Fig. S5 Ac magnetic susceptibility measurements for **1** (a) in zero static field. Frequency dependence of χ''_M susceptibilities for **1** (b) under different dc fields.

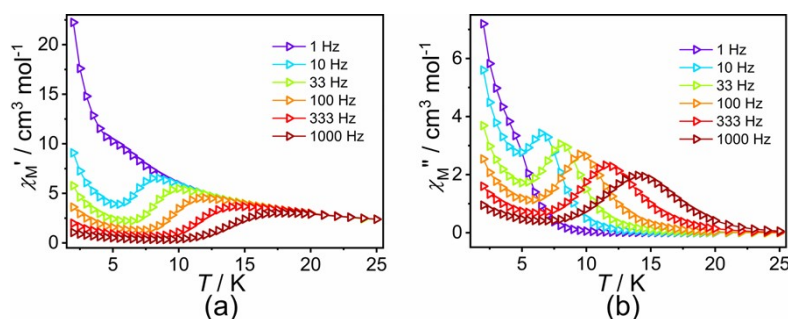


Fig. S6 Temperature dependence of the χ'_M (a) and χ''_M (b) ac susceptibilities for complex **2** at different frequencies under zero static field.

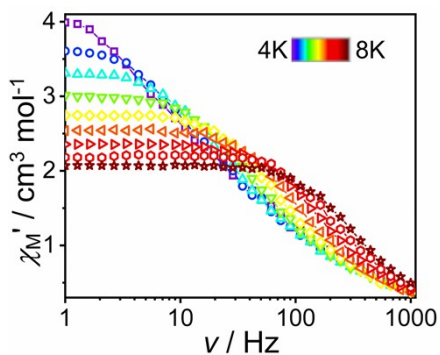


Fig. S7 Frequency dependence of the χ'_M ac susceptibilities for **1@Y** under zero static field.

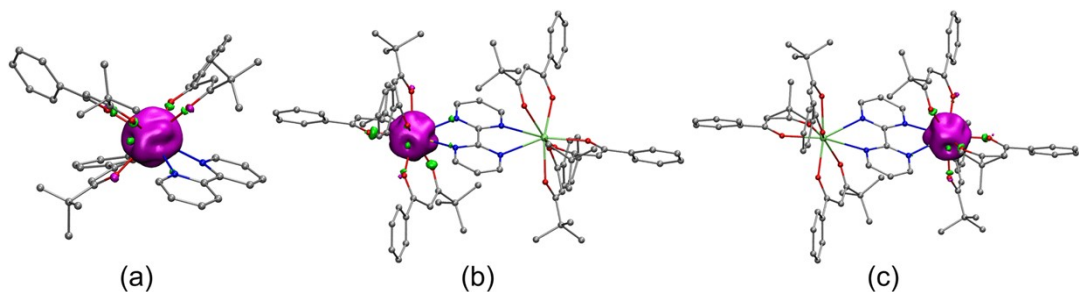


Fig. S8 Mulliken spin density of complexes **1** (a), **2a** (b) and **2b** (c) (magenta for α spin, green for β spin, isovalue = 0.02).

References:

- I. Fdez. Galván, M. Vacher, A. Alavi, C. Angeli, F. Aquilante, J. Autschbach, J. J. Bao, S. I. Bokarev, N. A. Bogdanov, R. K. Carlson, L. F. Chibotaru, J. Creutzberg, N. Dattani, M. G. Delcey, S. S. Dong, A. Dreuw, L. Freitag, L. M. Frutos, L. Gagliardi, F. Gendron, A. Giussani, L. González, G. Grell, M. Guo, C. E. Hoyer, M. Johansson, S. Keller, S. Knecht, G. Kovačević, E. Källman, G. Li Manni, M. Lundberg, Y. Ma, S. Mai, J. P. Malhado, P. Å. Malmqvist, P. Marquetand, S. A. Mewes, J. Norell, M. Olivucci, M. Oppel, Q. M. Phung, K. Pierloot, F. Plasser, M. Reiher, A. M. Sand, I. Schapiro, P. Sharma, C. J. Stein, L. K. Sørensen, D. G. Truhlar, M. Ugandi, L. Ungur, A. Valentini, S. Vancoillie, V. Veryazov, O. Weser, T. A. Wesołowski, P.-O. Widmark, S. Wouters, A. Zech, J. P. Zobel and R. Lindh, *J. Chem. Theory Comput.*, 2019, **15**, 5925-5964.
- W. Humphrey, A. Dalke, K. Schulten, VMD: visual molecular dynamics, *J. Mol. Graph.*, 1996, **14**, 33-38.
- B. O. Roos, R. Lindh, P.-Å. Malmqvist, V. Veryazov, P.-O. Widmark and A. C. Borin, *J. Phys. Chem. A*, 2008, **112**, 11431-11435.
- B. O. Roos, R. Lindh, P.-Å. Malmqvist, V. Veryazov and P.-O. Widmark, *J. Phys. Chem. A*, 2004, **108**, 2851-2858.
- S. Grimme, *WIREs Comput. Mol. Sci.*, 2011, **1**, 211-228.
- F. Neese, F. Wennmohs, U. Becker and C. Ripplinger, *C. J. Chem. Phys.*, 2020, **152**, 224108.
- F. Neese, ORCA-an ab initio, density functional and semiempirical Program Package, 5.0.3, University of Bonn, Bonn, Germany, 2022.
- A. D. Becke, *Phys. Rev. A*, 1988, **38**, 3098-3100.
- D. Aravena, F. Neese and D. A. Pantazis, *J. Chem. Theory Comput.*, 2016, **12**, 1148-1156.
- F. Weigend and R. Ahlrichs, *Phys. Chem. Chem. Phys.*, 2005, **7**, 3297-3305.
- C. Jin, X.-L. Li, Z. Liu, A. Mansikkämäki and J. Tang, *Dalton Trans.*, 2020, **49**, 10477-10485.